2021 43rd Annual International Conference of the
IEEE Engineering in Medicine & Biology Society (EMBC)
Oct 31 - Nov 4, 2021. Virtual Conference

Adapting the Finetech-Brindley Sacral Anterior Root Stimulator for Bioelectronic Medicine*

Felix Peterken[1], Moaad Benjaber[1,3], Sean Doherty[2], Tim Perkins[2],
Graham Creasey[5], Nick Donaldson[2], Brian Andrews[4], Timothy Denison[1,3]

***Abstract*—The Finetech-Brindley Sacral Anterior Root Stimulator (SARS) is a low cost and reliable system. The architecture has been used for various bioelectric treatments, including several thousand implanted systems for restoring bladder function following spinal cord injury (SCI). Extending the operational frequency range would expand the capability of the system; enabling, for example, the exploration of eliminating the rhizotomy through an electrical nerve block. The distributed architecture of the SARS system enables stimulation parameters to be adjusted without modifying the implant design or manufacturing. To explore the design degrees-of-freedom, a circuit simulation was created and validated using a modified SARS system that supported stimulation frequencies up to 600 Hz. The simulation was also used to explore high frequency (up to 30kHz) behaviour, and to determine the constraints on charge delivered at the higher rates. A key constraint found was the DC blocking capacitors, designed originally for low frequency operation, not fully discharging within a shortened stimulation period. Within these current implant constraints, we demonstrate the potential capability for higher frequency operation that is consistent with presynaptic stimulation block, and also define targeted circuit improvements for future extension of stimulation capability.**

I. Introduction

Emptying the bladder without a catheter, maintaining fecal continence, and restoration of sexual function are top priorities for Spinal Cord Injury (SCI) patients [1]. The Finetech-Brindley Sacral Anterior Root Stimulator (SARS) allows for independent micturition, defaecation, and penile erections [2]. The use of the device can greatly reduce the cost of managing the neurogenic bladder and bowel [3]. The SARS system consists of passive implanted parts (receiver, cable and electrodes) and battery powered external parts (controller and transmitter block), as illustrated in Fig. 1. To use, the patient selects a predetermined setting on the controller, which generates a defined stimulation pattern, and holds the transmitter block against the receiver, which sits under the skin on the abdomen and is connected to the electrodes placed on the S2-4 nerves, to stimulate micturition, defaecation or penile erection.

*Finetech Medical Ltd supplied the prototyping materials, but provided no other financial support for the project. Timothy Denison is <1% shareholder in Bioinduction Ltd, which is a majority owner of Finetech Medical Ltd. Sean Doherty is serving a secondment with Finetech Medical Ltd funded by innovate UK.

[1]University of Oxford; [2]University College, London; [3]MRC Brain Network Dynamics Unit; [4]Nuffield Department of Surgical Sciences; [5]Stanford University.

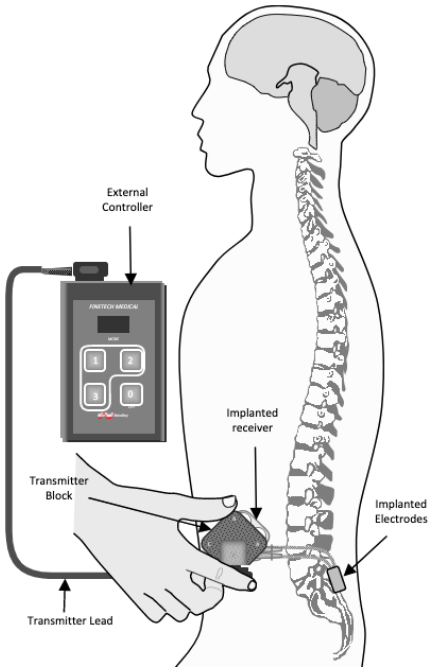

Fig. 1: *Diagram for the Finetech-Brindley SARS system. (Ref Finetech Medical, used with permission)*

Having a passive receiver comes with a number of benefits: 1) it can be less complex to produce; 2) it requires no software inside of the implant, as the stimulation characteristics are controlled by the transmitter waveform ; 3) no batteries are required in the implant, which can help avoid replacement surgery; 4) it supports reliable chronic use, with a mean time-to-failure previously found to be 19.6 years [4]. As the SARS system nears its fortieth anniversary of being commercially available some early patients continue to be supported through their forth decade of use.

For SARS, the system is typically 2 or 3 channels, different channels run on 7 and 9 MHz (with the 3 channel system having two 9 MHz coils), and control different electrodes. Electrodes are placed on the S2, S3 and S4 nerves and are either intrathecal "book end" electrodes, which enclose the sacral roots, or extradural electrodes, which are located alongside the mixed sacral nerves. With conventional stimulation paradigms, the small diameter parasympathetic fibres innervating the detrusor cannot be activated without simultaneous stimulation of the larger somatic fibres innervating External

Urethral Sphincter (EUS), prohibiting natural voiding. Therefore the temporal differences between smooth and striated muscle are exploited to allow post-stimulus voiding to occur, where the slower relaxation of the detrusor creates a pressure differential after a period of stimulation resulting in building pressure and a bursting micturition pattern.

A. Motivation for Extending Stimulation Capabilities

Sacral sensory nerve rhizotomy usually accompanies the operation to implant the Finetech-Brindley SARS system. This eliminates neurogenic detrusor overactivity (NDO) and detrusor sphincter dysynnergia (DSD), thus significantly improving continence, reducing residual urine volumes and reducing autonomic dysreflexia [6] [7] [8]. NDO and DSD arise from pathological reflexes present following SCI, and cutting of the posterior roots effectively blocks this reflex arc. However, rhizotomy also abolishes reflex sexual function and residual pelvic sensation present in some with SCI. For SARS, low-frequency stimulation of the posterior sacral roots can modulate NDO effectively, however, DSD continues to impair voiding [9]. The potential for reversible blocks to stop unwanted afferent activity and mitigate rhizotomy has motivated this design study.

Expanding stimulation capability might help with other conditions as well. Several devices have gone on to use the SARS architecture effectively for other conditions. These include restoration of cough function following cervical SCI [10], tibial nerve stimulation for those with overactive bladder [11], and functional electrical stimulation of drop foot for improved walking [12]. The simple, low-cost architecture of the SARS system, together with the passive receiver, make it a highly configurable platform for bioelectronic medicine; coupled with the long-term safety data, it is a desirable architecture worth consideration for several applications. This design study explored what might be achievable without changes to the existing CE-marked implantable receiver, and focusing only on modification of the external transmitter as a research tool.

B. Target Specifications

This design study is focused specifically on extending the capability of the SARS system to deliver charge at higher frequencies. To enact a reversible nerve block, the implant would have to deliver pulses at much higher frequencies than it currently operates. Differential blocking between the detrusor and sphincter could be achieved by exploiting the fact that the larger diameter somatic fibres are activated at a lower threshold than the thinner autonomic fibres, hence somatic activity could be blocked at a lower threshold [18].

TABLE I: *Blocking Specifications taken from literature using different electrodes and nerves.*

Site	Local to Electrode	Presynaptic
Frequency (kHz)	5 - 10	0.6
Charge/phase (nC)	80 - 1000	30 - 250
Waveform	Biphasic	Monophasic
References	[13][14][15]	[16][17]

The presynaptic block uses a monophasic square wave of 600 Hz, with pulse widths ranging from 30 - 500 μs and delivering 27 - 250 nC per pulse [16]. A more recent study in dogs achieves a 56% reduction in external urethral sphincter pressure whilst maintaining 96% of the detrusor pressure by using 60 μs pulses and delivering 66 - 78 nC of charge per pulse [19].

The high frequency localised block uses a charge balanced biphasic waveform with an amplitude and frequency in excess of 1 V and 1 kHz. However this would cause a prolonged onset response, which would be diminished if higher frequencies were used [20]. The more commonly used value for *in vivo* systems is 10 kHz to reduce this onset response, but 5 kHz has been used as well [13] [14]. This is orders of magnitude above the current settings in the SARS device. We have limited the focus of this study to achieving the medium frequency presynaptic block requirements.

The design specifications (Table I) are intended to guide our work but there are caveats, namely these values were taken from literature across several nerves (of varying axon diameters), species, and electrodes, so further clinical validation at the proposed nerve block site will be required to determine the specific thresholds.

II. Electrical Principles of Operation

The circuitry of the SARS system is shown in Figure 2. The principle of operation is to generate a high-frequency, amplitude modulated signal that is inductively coupled across the skin; the received signal is then rectified and low-pass filtered to provide a stimulation pulse. In the existing SARS design, the external transmitter is controlled by V_{in}, which is a square wave of duration 24 - 720 μs at 8 - 46 Hz in the current system [21]. When switched on, the Hartley Oscillator generates a high frequency carrier from the resonance between L, M, N and C_1. The frequency of oscillation is determined by $f_r = \left(2\pi\sqrt{L_{tot}C}\right)^{-1}$. For the simulation, L_{tot} was the total inductance on the transmitter circuit, calculated from the resonant frequency and apportioning the values of L, M , and N according to the square of the turns ratio. The inductors are coupled through the skin to T on the implant [5].

The implant rectifies this signal and provides stimulation through the electrodes. The voltage induced in T is a 7 or 9 MHz oscillation and the negative envelope of this signal is obtained with the 1N914 diode rectifier, and the low pass filter created by C_5 and R_2. The resulting signal is a square wave at node g on Figure 2. The larger C_6 blocking capacitor ensures charge balance across the electrode; for the purposes of simulation and bench testing, we modelled the electrode as a 470 Ω resistor [18].

The blocking capacitor can prevent effective stimulation at higher frequencies. During a stimulation pulse, V_p, charge

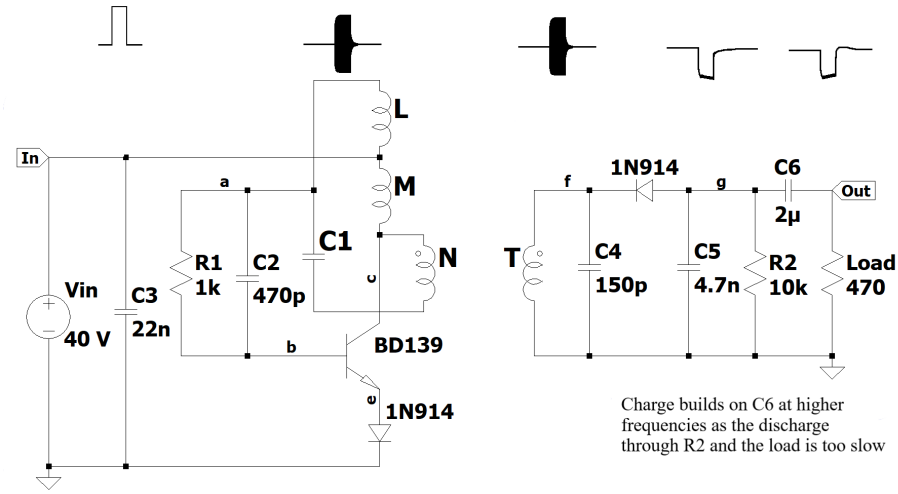

f_r (MHz)		7	9
C_1 (pF)		470	270
L	nH	79	64
	n_t	1	1
M	nH	314	64
	n_t	2	1
N	nH	707	1024
	n_t	3	4
T	nH	7861	4117
	n_t	10	8

Fig. 2: *Circuit Diagram for the Finetech-Brindley SARS system [5], and component values used in the circuit simulation. This produces 7/9 MHz oscillations when ignoring the mutual inductance and coil self-capacitance between L, M and N. The coupling constant between N and T was $k = 0.15$ in the simulation, but it is likely to be lower when the coils are implanted. Charge building across C_6 is the limiting factor to delivering charge at higher frequencies.*

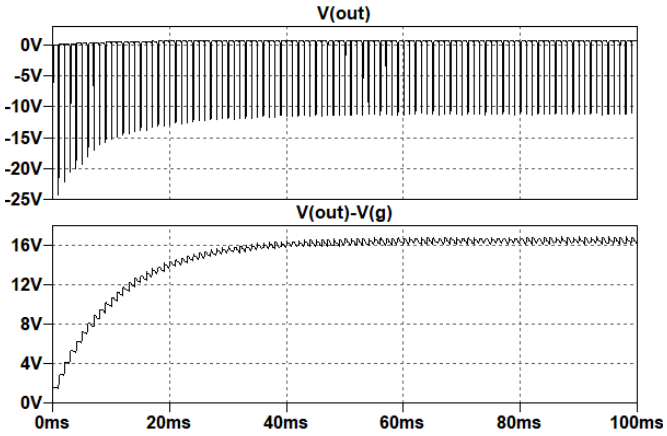

Fig. 3: *Spice simulation at 1 kHz and 65 µs pulses. At frequencies above those used in the existing design, C_6 retains a significant amount of charge between pulses.*

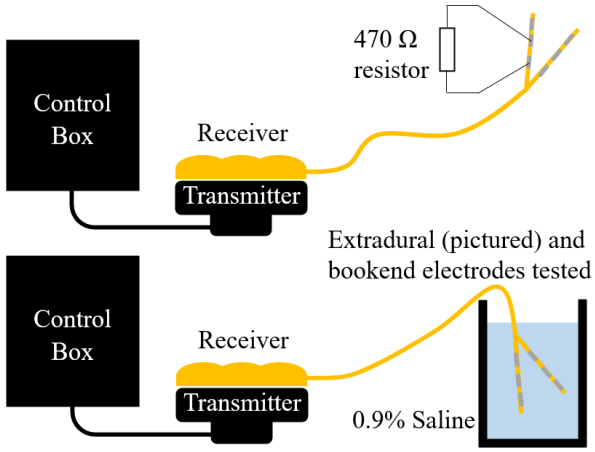

Fig. 4: *Experimental set up for collecting results with a resistor and with electrodes in saline. The Receiver was placed on the transmitter to prevent any changes in coupling constant between experiments.*

builds up on the capacitor C_6, which appears as a decrease in voltage magnitude across the load. After the pulse, C_6 discharges, which appears as a small positive voltage across the load. In the existing design, the capacitor can mostly discharge between the pulses so the effect on the subsequent pulse is negligible. However, at the higher frequencies, C_6 accumulates charge, which can be seen in the simulation in figure 3. This means at higher frequencies, the pulse amplitude is decreased as the capacitor has less time to discharge between the pulses, and the residual voltage acts in superposition to lower the stimulation voltage applied to the electrode. This also leads to the build up of the inter-pulse residual voltage, V_d, with increasing frequency and pulse duration, that is shared across the electrode and the discharge resistor R_2.

III. Characterization Methods

The circuit was characterised using the magnitudes of the pulse amplitude and discharge voltage, which are shown in Figure 5. The system was recreated on the test bench as shown in Figure 4. A simulation of the circuit was also created using the values in Figure 2 in SPICE (LTspice XVII(x64), version 17.0.017, 2020), to probe the behaviour of the circuit at higher frequencies and at all the nodes in the circuit. The coupling constant was taken as $k = 0.15$ [22]. During the validation tests, the receiver was placed on top of the transmitter to ensure consistent coupling constant between trials. This resulted in a higher coupling co-efficient

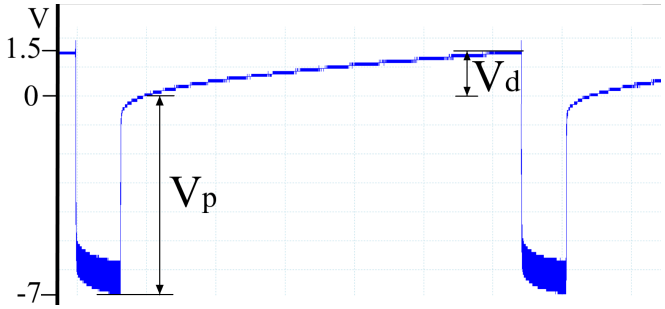

Fig. 5: *An example oscilloscope trace of voltage across the extradural electrode in saline, with pulse and discharge voltages labelled.*

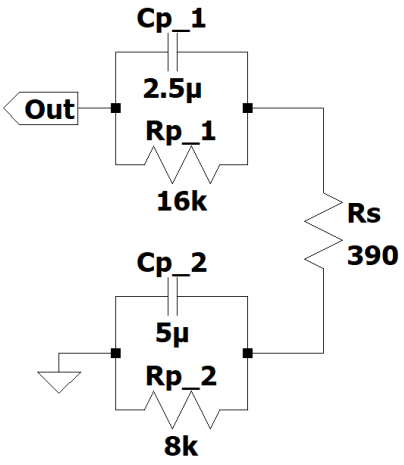

Fig. 6: *Electrode model adapted from Donaldson* et al, *2003 [23]. P_1 refers to the positive pole, p_2 refers to the two negative poles. R_s was decreased to match the characteristics seen with bench testing.*

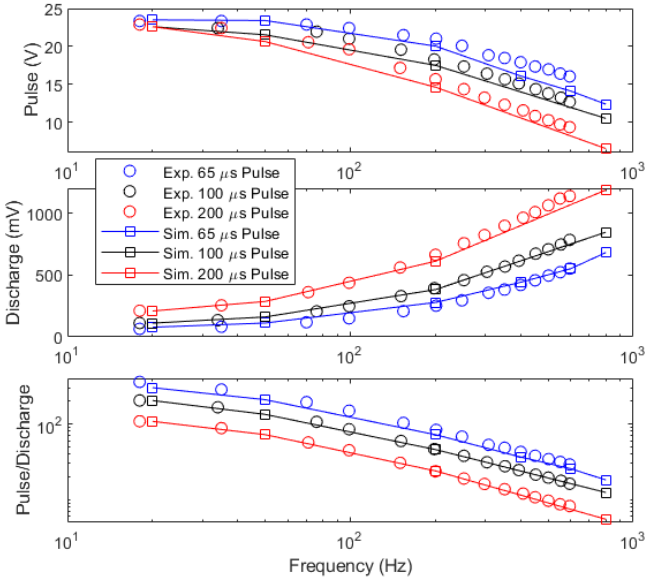

Fig. 7: *Behaviour of system with 470 Ω load across the electrodes on bench test (exp.) and in the simulation (sim.) at different pulse widths and frequencies.*

than would be present in the implanted device, which could be as low as $k = 0.01$, but the principles explored remain valid.

To validate the simulation results at intermediate frequencies, a modified analogue SARS system, adapted to produce frequencies between 35 and 593 Hz (Tim Perkins, University College London) was used. The modified device limited pulse width and height to avoid additional power dissipation in the existing (1979) transmitter design which could cause heating when operated well above the original maximum stimulation frequency of 46Hz. Using design criteria from Donaldson and Perkins [22] a 4.7-times more power efficient RF transmission link has proved possible, which would allow correspondingly higher stimulation frequencies to be used more safely.

For these tests, the transmitter was set to the maximum voltage. The voltage was initially taken across a 470 Ω resistor for set pulse widths and a range of frequencies. Voltages were measured at steady state. The voltages were also measured when the electrodes submerged in 0.9% saline solution to mimic the conditions *in vivo*. The load to match the electrode model was adapted from Donaldson *et al*, 2003 [23], with the saline resistance changed to match the results gathered (fig. 6).

IV. Characterization Results

Figure 7 shows the expected relationship of the pulse amplitude decreasing with higher frequencies and longer pulses, from the increase in charge stored on the DC blocking capacitor. The discharge voltage increases accordingly as the charge dissipates from the capacitor quicker. The simulation showed general agreement for these parameters, allowing for tentative extrapolation to higher frequencies.

For the electrodes in saline, the pulse amplitude exhibits a similar characteristic but at a lower voltage. Figure 8 compares the resistor with electrodes immersed in saline and also shows the results from simulation with the equivalent electrode model, with the saline resistance set to 390 Ω. This shows acceptable agreement with the book end electrodes in saline. After implantation, the impedance of the electrode tends to increase [24], so the 470 Ω may be a more accurate representation of the implanted system. The waveform for the discharging phase in saline varied from that of the resistor however, and had a larger residual voltage, which is more similar in the equivalent electrical model.

Given assumptions in the model, V_p normalised by V_d can correct for discrepancies between tests and inaccuracy of tuning the input. For example, the incorrect coupling constant or a lower input voltage on the simulation would result in a reduction in V_p and the same proportional reduction in V_d. The simulation shows very good agreement on this parameter

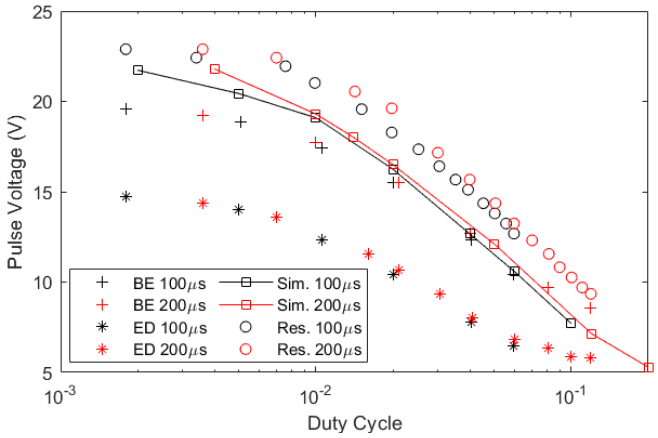

Fig. 8: *Comparison between the 470 Ω resistor model, the two electrodes (BE - Book end, ED - Extradural) submerged in saline, and the equivalent electrical model of the book end electrode (Sim.)*

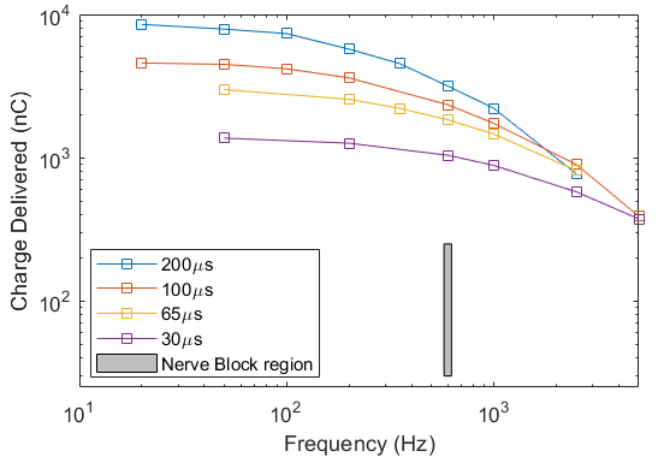

Fig. 9: *Simulated behaviour of the charge delivered during a pulse. The input voltage can be decreased to meet the charge requirements of the nerve block, shown as the shaded region.*

for the resistor tests, suggesting that the discrepancies of the pulse amplitude and discharge voltage can be corrected for by fine tuning the input voltage if such accuracy was required.

V. Discussion

A. Suitability for Synaptic Blocks

By modifying the transmitter design, the existing SARS receiver appears capable of delivering intermediate stimulation levels needed for a presynaptic block. The charge delivered per pulse was calculated by integrating the current through the load over the duration of the pulse, with the growth time on every pulse taken into consideration. When comparing the charge delivered (in fig. 9) against the blocking criteria in section I-B, the presynaptic block appears to be feasible for the bookend electrode as the charge delivered is comfortably above that used in previous studies, so should be able to be used on an implanted system [16][17][25]. Further work would need to be done to determine the conditions for maximum difference in detrusor and sphincter response which are specific to the electrodes and the site used in the SARS system, but this shows promise in providing an extension to the capability of the FineTech-Brindley SARS system.

B. Limitations

The approach might still have limitations. If the presynaptic block is effective, it could prevent DSD if an amplitude can be found for reduced contraction of the sphincter whilst maintaining the contraction of the detrusor [19]. However, the rhizotomy does present other benefits which could not be achieved with this form of block, like reducing NDO and autonomic dysreflexia. This motivates the exploration of even higher stimulation frequencies.

Higher frequency stimulation capability raises design considerations that require further consideration. From a functional standpoint, we must address the significant attenuation of the output signal from the charge accumulated on the DC blocking capacitor when operating at frequencies required for the localised nerve block. In addition, the power dissipated must be also considered at higher frequencies. This would cause the temperature of the implant and transmitter to rise, warranting further study to ensure that this remains within a safe operating range. Finally, the coupling constant used in this study is an optimistic value when considering an implanted system, which would lead to a drop in efficiency and further heating to achieve the same output.

C. Potential Mitigations

While the localised high frequency block does not appear to be feasible when extrapolating using the simulation, there are focused design changes which might extend the operating range of the SARS receiver at the expense of design changes to the implant, requiring regulatory approvals. The aim is to increase the charge delivered and the voltage at the electrode at higher frequencies. Optimizing the time constants of the receiver is a first mechanism to explore. As C_6 discharges through both R_2 and the load, decreasing R_2 will decrease the charge stored on the capacitor, and should increase the output voltage. Investigation of the optimal value of R_2 for higher frequency operation is ongoing, but preliminary results show that the power in the transmitter will also need to be increased, and so in parallel a temperature management strategy might be required. Ideally, R_2 would be dynamic, being high during the pulse phase to preserve the effectiveness of the rectifier, and low during the discharging phase, to discharge C_6 quicker. These competing constraints can be met in active systems for stimulation, but at the expense of added complexity and failure modes.

VI. Conclusion

The existing SARS circuit architecture was studied to understand how it might support extended stimulation fre-

quency. The system was modeled in SPICE, including electrode interfaces, which simulated the behaviour at frequencies required for a localised nerve block as well as baseline performance used today. To validate this model, a modified analogue SARS system was created to deliver stimulation up to 600 Hz. Based on this model, the electrical conditions to implement a presynaptic block appear to be feasible with the modified system prototype.

The model and bench validation also highlighted areas for further improvement. Specifically, the charge being delivered to the electrode can be limited by the transient dynamics of the blocking capacitor; this effect can be a major limitation for delivering charge at higher frequencies. A method of refining the design of the receiver to account for these dynamics is likely feasible, based on optimization of time constants, as long as the heating in the transmitter can also be addressed.

In summary, the flexibility and modularity of the SARS design could enable a variety of bioelectronic therapies through adjustment of the external transmitter, while minimizing or avoiding design changes in the implantable receiver. In the short term, these results support a clinical investigation to demonstrate that the extended stimulation capability can enable a presynaptic block of the target nerves as predicted, which leverages the latent capability of the existing SARS implant architecture.

VII. Disclosures

Sean Doherty is on a secondment to Finetech Medical Ltd through a grant from the Royal Academy of Engineering. Tim Denison has shares in Bioinduction Ltd, who has a controlling interest in Finetech Medical.

References

[1] Dennis Bourbeau, Abby Bolon, Graham Creasey, et al. Needs, priorities, and attitudes of individuals with spinal cord injury toward nerve stimulation devices for bladder and bowel function: a survey. *Spinal Cord*, 2020.

[2] F.M.J. Martens and J.P.F.A. Heesakkers. Clinical results of a brindley procedure: Sacral anterior root stimulation in combination with a rhizotomy of the dorsal roots. *Advances in Urology*, 2011.

[3] Graham H Creasey and John E Dahlberg. Economic consequences of an implanted neuroprosthesis for bladder and bowel management. *Archives of physical medicine and rehabilitation*, 82(11):1520–1525, 2001.

[4] Giles Brindley. The first 500 sacral anterior root stimulators: implant failures and their repair. *Paraplegia*, 33:5–9, 1995.

[5] T.A. Perkins and N.J. Chaffey. Practical problems of controlling medical implants via radio link. In *A Handbook on Biotelemetry and Radio Tracking*, pages 487 – 494, 1979.

[6] Markus Hohenfellner, Jürgen Pannek, et al. Sacral bladder denervation for treatment of detrusor hyperreflexia and autonomic dysreflexia. *Urology*, 58(1):28 – 32, 2001.

[7] L. Baskin and R Schmidt. Bladder rehabilitation with dorsal rhizotomy and ventral neuroprosthesis. *Spinal Cord*, 1992.

[8] J.R. Vignes, L. Bauchet, and F. Ohanna. Urodynamic observations on patients with sacral anterior root stimulators. In D.E. Sakas, B.A. Simpson, and E.S. Krames, editors, *Operative Neuromodulation. Acta Neurochirurgica Supplements*. Springer, Vienna, 2007.

[9] A. Kirkham, S. Knight, M. Craggs, et al. Neuromodulation through sacral nerve roots 2 to 4 with a finetech-brindley sacral posterior and anterior root stimulator. *Spinal Cord*, 40:272–281, 2002.

[10] Anthony F. DiMarco et al. Lower thoracic spinal cord stimulation to restore cough in patients with spinal cord injury: Results of a national institutes of health–sponsored clinical trial. *Arch Phys Med Rehabil*, 90:715–725, 2009.

[11] D.A. Janssen, F. Farag, and J.P. Heesakkers. Urgent-sq implant in treatment of overactive bladder syndrome: 9-year follow-up study. *Neurourology and Urodynamics*, 32:472–475, 2013.

[12] L. Kenny et al. An implantable two channel drop foot stimulator: Initial clinical results. *Artificial Organs*, 26(3):267–270, 2002.

[13] Wenbin Guo et al. Restoring both continence and micturition after chronic spinal cord injury by pudendal neuromodulation. *Experimental Neurology*, page 113658, 2021.

[14] Amol Soin, Nemath Syed Shah, and Zi-Ping Fang. High-frequency electrical nerve block for postamputation pain: a pilot study. *Neuromodulation: Technology at the Neural Interface*, 18(3):197–206, 2015.

[15] N. Bhadra, N. Bhadra, K. Kilgore, and K.J. Gustafson. High frequency electrical conduction block of the pudendal nerve. *J Neural Eng*, 3(2):180–187, 2006.

[16] M Solomonow, E Eldred, J Foster, and J Lyman. A new technique for functional neuromuscular stimulation. In *Advances on External Control of Human Extremities*, pages 47–62. Yugoslav Committee for Electronics and Automation, 1978.

[17] HS Shaker, LM Tu, S Robin, K Arabi, M Hassouna, M Sawan, and MM Elhilali. Reduction of bladder outlet resistance by selective sacral root stimulation using high-frequency blockade in dogs: an acute study. *The Journal of urology*, 160(3 Part 1):901–907, 1998.

[18] Giles Brindley et al. Sacral anterior root stimulators for bladder control in paraplegia. *nature*, 1982.

[19] M Abdel-Gawad, S Boyer, M Sawan, and MM Elhilali. Reduction of bladder outlet resistance by selective stimulation of the ventral sacral root using high frequency blockade: a chronic study in spinal cord transected dogs. *The Journal of urology*, 166(2):728–733, 2001.

[20] Niloy Bhadra and Kevin L Kilgore. High-frequency electrical conduction block of mammalian peripheral motor nerve. *Muscle & Nerve: Official Journal of the American Association of Electrodiagnostic Medicine*, 32(6):782–790, 2005.

[21] FineTech Medical Ltd. *Clinician Manual*. Welwyn Garden City, Hertfordshire, England.

[22] N. Donaldson and T.A. Perkins. Analysis of resonant coupled coils in the design of radio frequency transcutaneous links. *Medical and Biological Engineering and Computing*, 1983.

[23] N de N Donaldson, L Zhou, TA Perkins, M Munih, M Haugland, and Thomas Sinkjaer. Implantable telemeter for long-term electroneurographic recordings in animals and humans. *Medical and Biological Engineering and Computing*, 41(6):654–664, 2003.

[24] PEK Donaldson, N Donaldson, DN Rushton, and TA Perkins. Estimated electrode operating conditions of the first london mk v implanted stimulator. *Journal of Medical Engineering and Technology*, 22(2):259–263, 1999.

[25] E. Eldred and M. Solomonow. Effects of high-frequency (500-l ,000 hz), indirect stimulation on slow and fast muscle relevant to orthotic applications. *Journal of Electromyography and Kinesiology*, 2(3), 1992.